Block Diagonalization Precoding and Signal Detection for Spatial Multiplexing MIMO Systems

by

Ali Alwalid
B.Sc., Misurata University, Misurata, Libya, 2010

A Report Submitted in Partial Fulfillment
of the Requirements for the Degree of

MASTER OF ENGINEERING

in the Department of Electrical and Computer Engineering

Supervisory Committee

Dr. T. Aaron Gulliver, Supervisor

(Department of Electrical and Computer Engineering)

Dr. Hong-Chuan Yang, Departmental Member

(Department of Electrical and Computer Engineering)

Abstract

Spatial multiplexing (SM) multi-input multi-output (MIMO) systems can transmit independent data streams using multiple antennas to achieve high data rates. SM techniques can be employed in single-user multi-input multi-output (SU-MIMO) and multi-user multi-input multi-output (MU-MIMO) systems. There are two types of interference in SM MIMO systems, inter-antenna interference and multi-user interference (MUI). In order to improve SM MIMO system performance, channel precoding is used at the base station (BS). In this report, block diagonalization (BD) channel precoding is employed to reduce the MUI and decompose the MU-MIMO system into parallel SU-MIMO systems. Then, several detection techniques are used to detect the received signal and reduce the inter-antenna interference at each user. Simulation results are presented to evaluate and compare the bit error rate (BER) performance of SU-MIMO and MU-MIMO systems with zero-forcing (ZF), minimum mean square error (MMSE), ordered successive interference cancellation (OSIC), and maximum likelihood (ML) detection algorithms. Three modulation schemes, namely QPSK, 16 QAM and 64 QAM are considered. Further, the BER performance of MIMO systems in correlated channels is investigated using the exponential correlation model.

Table of Contents

List of Figures

List of Tables

Acknowledgments

First of all, I would to express my deepest thanks to my supervisor Dr. T. Aaron Gulliver for his invaluable advice and comments. His guidance and consistent encouragement allowed me to complete this work. I would also like to thank Dr. Hong-Chuan Yang for being on my supervisory committee and for providing useful knowledge in the field of wireless communication systems during my academic program. Finally, I thank my family, my friends and the staff of the Department of Electrical and Computer Engineering for their support, patience and motivation through my studies.

Glossary

AWGN	Additive white Gaussian noise
BD	Block diagonalization
BER	Bit error rate
BS	Base station
CSI	Channel state information
DPC	Dirty paper coding
FDD	Frequency division duplex
FLOPs	Floating point operations
IEEE	Institute of Electrical and Electronics Engineers
MATLAB	Matrix laboratory
MIMO	Multi-input multi-output
ML	Maximum likelihood
MMSE	Minimum mean square error
MUI	Multi-user interference
MU-MIMO	Multi-user multi-input multi-output
OSIC	Ordered successive interference cancellation
QAM	Quadrature amplitude modulation
QPSK	Quadrature phase shift keying
SD	Sphere decoding
SIC	Successive interference cancellation
SINR	Signal-to-interference plus noise ratio
SISO	Single-input single-output
SM	Spatial multiplexing
SM MIMO	Spatial multiplexing multi-input multi-output
SNR	Signal-to-noise ratio
SU-MIMO	Single-user multi-input multi-output

TDD	Time division duplex
THP	Tomlinson-Harashima precoding
UE	User equipment
ZF	Zero-forcing

1 Introduction

Due to the dramatic increase in mobile network data traffic, multi-input multi-output (MIMO) systems have become crucial for future wireless networks. Multiple antennas are employed at the base station (BS) and the user equipment (UE) in MIMO systems. MIMO systems have more degrees of freedom than single-input single-output (SISO) systems which can increase wireless system capacity and offer more reliable communications [4], [17]. The capacity of MIMO channels increases linearly with the minimum number of transmit and receive antennas without requiring increased signal power and bandwidth [1]. The use of MIMO technology it also increases the complexity of wireless networks. Many standards such as IEEE802.16 and IEEE802.11n employ MIMO technology [2].

Spatial diversity (SD) or spatial multiplexing (SM) techniques can be employed in MIMO systems for data transmission. SD uses multiple antennas to transmit multiple copies of the transmitted data stream. It can improve transmission reliability and the bit error rate (BER) performance. SM divides the data stream into several independent data streams which are modulated and transmitted simultaneously from multiple transmit antennas. These antennas should be sufficiently separated to reduce the correlation between neighboring antennas [17]. SM technology can increase the channel capacity without requiring additional bandwidth. In [24], it was shown that employing SM in MIMO systems increases the system capacity.

SM can be employed in single-user MIMO (SU-MIMO) systems and multi-user MIMO (MU-MIMO) systems. In MIMO systems, there are two types of interference, inter-antenna interference and multi-user interference. Inter-antenna interference is the interference between antennas for the same user. On the other hand, multi-user interference (MUI) is between the data streams of multiple users. MUI can be reduced by using channel precoding techniques at the BS [15]. Several detection techniques and channel precoding algorithms have been proposed to reduce the effects of inter-antenna interference and multi-user interference, respectively [17]. In the next two subsections, a review of several detection and precoding techniques is presented.

1.1 SM MIMO Detection

In order to achieve high data rates and low bit error rates, SM MIMO detection techniques are used to reduce inter-antenna interference. In [16], a low complexity MIMO receiver was presented to mitigate inter-antenna interference. Several SM MIMO detection techniques were discussed and evaluated in [3] in terms of their BER performance and computational complexity. Channel state information (CSI) is required at the UE to implement these techniques. In this report, zero-forcing (ZF), minimum mean square error (MMSE), ordered successive interference cancellation (OSIC), and maximum likelihood (ML) detection techniques are considered.

1.2 MIMO Channel Precoding

Channel precoding plays an essential role in improving MIMO system reliability. In the downlink MU-MIMO channel, MUI is introduced when a single BS communicates with multiple users due to the interference between the transmitted data streams. MIMO channel precoding is used to reduce this MUI. The BS has higher computational capabilities than the UE so the channel precoding is usually applied at the BS. Several precoding techniques have been proposed such as channel inversion, regularized channel inversion, block diagonalization, regularized block diagonalization, dirty paper coding, and Tomlinson-Harashima precoding [17]. Further research has been done to improve existing precoding algorithms in terms of BER performance and complexity [12], [14], [26].

In order to perform channel precoding, CSI is required at the BS. There are several ways to obtain this CSI. In time division duplex (TDD) systems, the BS can exploit the channel reciprocity and make channel measurements based on the received signal because the downlink and uplink channels share the same frequency band to transmit and receive signals. In frequency division duplex (FDD) systems, there is no channel reciprocity because the downlink and uplink channels are on different frequencies, so the CSI is estimated and fed back from the user to the

BS [6], [17].

In [18], [22], block diagonalization (BD) precoding was proposed for MU-MIMO systems. Employing BD precoding at the BS decomposes the MU-MIMO system into parallel SU-MIMO systems to reduce the MUI. BD has better performance compared with simple channel inversion precoding and lower complexity than non-linear precoding techniques such as dirty paper coding (DPC) and Tomlinson-Harashima precoding (THP) [8], [17]. Thus in this report, BD precoding is considered.

1.3 Objectives and Methodology

The detection techniques given in Section 1.1 for SM MIMO systems are compared in terms of their BER performance. MIMO systems with different numbers of antennas are evaluated, and three modulation schemes, namely QPSK, 16 QAM and 64 QAM, are considered [3], [8], [21]. BD channel precoding is used to reduce the effect of MUI in MU-MIMO systems [11], [15], [17]. Moreover, the BER performance of MIMO systems is investigated over correlated channels [8].

The objective is to evaluate the BER performance of SU-MIMO and MU-MIMO systems. For the downlink SU-MIMO channel, it is assumed that a single BS communicates with a single user. The BS and UE are equipped with N_B and N_U antennas, respectively. At the BS, the data is divided into several independent data streams, and then modulated and transmitted simultaneously from multiple antennas. No channel precoding is applied at the BS because there is no MUI. The ZF, MMSE, OSIC and ML techniques are used to detect the received signal and reduce the inter-antenna interference at the UE. The BER performance of these detection techniques is evaluated and compared.

For the downlink MU-MIMO channel, it is assumed that a single BS communicates with K users $k = 1, 2, \dots, K$. The BS is equipped with N_B antennas and each user is equipped with N_U antennas. BD channel precoding is employed at the BS to decompose the MU-MIMO system into parallel SU-MIMO systems and reduce the MUI. The ZF, MMSE, OSIC and ML techniques are used to detect the received signal and reduce the inter-antenna interference at each UE. The BER performance of these detection techniques is evaluated and compared. It is assumed

that full CSI is available at the BS and UE. An independent Rayleigh fading channel model is assumed, and the noise is additive white Gaussian noise (AWGN). MATLAB is used for the simulations.

1.4 Report Outline

Chapter 2 gives the SU-MIMO and MU-MIMO system models. The BD algorithm is presented and considered for channel precoding in MU-MIMO systems. The ZF, MMSE, OSIC and ML signal detection techniques are also presented. These techniques are studied and compared in terms of their computational complexity. Spatial correlation is also considered using an exponential correlation model. Chapter 3 presents the methodology and the simulation parameters used in the MATLAB simulation of the SU-MIMO and MU-MIMO systems. Simulation results are given and the performance of the detection techniques is discussed for both SU-MIMO and MU-MIMO systems. Chapter 4 provides some concluding remarks and discusses possibilities for future work.

Notation: in this report, uppercase bold letters denote matrices, while lowercase bold letters denote vectors. Lowercase letters donates scalars. $\boldsymbol{A}^T$ and $\boldsymbol{A}^H$ denote matrix transpose and Hermitian transpose, respectively.

2 MIMO Systems

This chapter provides the spatial multiplexing (SM) MIMO system models and the signal detection techniques. Spatial correlation is also discussed.

2.1 MIMO System Model

Downlink MIMO channel models for both SU-MIMO and MU-MIMO are considered. It is assumed that a single BS communicates with a single user for SU-MIMO and with multiple users for MU-MIMO. A SM MIMO system is considered.

2.1.1 SU-MIMO System Model

Figure 1 shows the SU-MIMO system model. A single BS equipped with N_B antennas communicates with a single user equipped with N_U antennas. $\boldsymbol{H}$ is the channel matrix between the BS and UE. The channel matrix can be expressed as [8]

$$\boldsymbol{H} = \begin{bmatrix} h_{1,1} & \cdots & h_{1,i} & \cdots & h_{1,N_B} \\ \vdots & \vdots & \vdots & \vdots & \vdots \\ h_{j,1} & \cdots & h_{j,i} & \cdots & h_{j,N_B} \\ \vdots & \vdots & \vdots & \ddots & \vdots \\ h_{N_{U,1}} & \cdots & h_{N_U,i} & \cdots & h_{N_U,N_B} \end{bmatrix} \qquad (1)$$

where $h_{j,i}$ denotes the channel gain between the ith transmit antenna at the BS and the jth receive antenna at the UE, $i = 1,2,\dots,N_B$, $j = 1,2,\dots,N_U$. The transmitted and received signal vectors are $\boldsymbol{x} = \left[x_1, x_2, \dots, x_i, \dots, x_{N_B}\right]^T$ and $\boldsymbol{y} = \left[y_1, y_2, \dots, y_j, \dots, y_{N_U}\right]^T$, respectively, where x_i denotes the transmitted signal at the ith transmit antenna and y_j denotes the received signal at the jth receive antenna. A narrowband flat fading channel is assumed so the received signal at a given time is independent of the received signals at other times [17]. The received signal at the UE can then be expressed as

$$\boldsymbol{y} = \boldsymbol{H}\boldsymbol{x} + \boldsymbol{z} \qquad (2)$$

where $\boldsymbol{z} = [z_1, z_2, \dots, z_j, \dots, z_{N_U}]^T$ and z_j denotes additive white Gaussian noise (AWGN) with zero mean and variance σ_z^2 at the jth receive antenna. From (1) and (2), the received signal can be expressed as

$$\begin{bmatrix} y_1 \\ \vdots \\ y_j \\ \vdots \\ y_{N_U} \end{bmatrix} = \begin{bmatrix} h_{1,1} & \cdots & h_{1,i} & \cdots & h_{1,N_B} \\ \vdots & \ddots & \vdots & \vdots & \vdots \\ h_{j,1} & \cdots & h_{j,i} & \cdots & h_{j,N_B} \\ \vdots & \vdots & \vdots & \ddots & \vdots \\ h_{N_{U,1}} & \cdots & h_{N_U,i} & \cdots & h_{N_U,N_B} \end{bmatrix} \begin{bmatrix} x_1 \\ \vdots \\ x_i \\ \vdots \\ x_{N_B} \end{bmatrix} + \begin{bmatrix} z_1 \\ \vdots \\ z_j \\ \vdots \\ z_{N_U} \end{bmatrix} \qquad (3)$$

Detection techniques to reduce the inter-antenna interference at the UE will be discussed in Section 2.2.

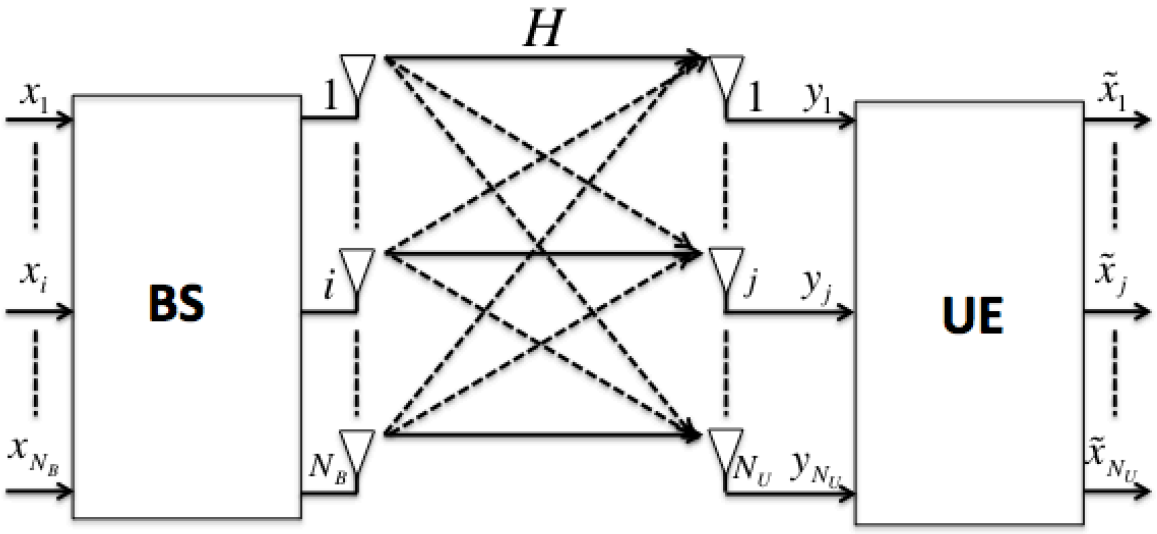

Figure 1: The single-user multi-input multi-output (SU-MIMO) system model.

2.1.2 MU-MIMO System Model

Figure 2 shows the MU-MIMO system model. A single BS equipped with multiple antennas communicates with K users, and each user is equipped with multiple antennas. Assuming that the K users have the same number of antennas. Let N_B and N_U denote the number of antennas at the BS and the kth UE, respectively. The total number of receive antennas is

$$N_R = KN_U \qquad (4)$$

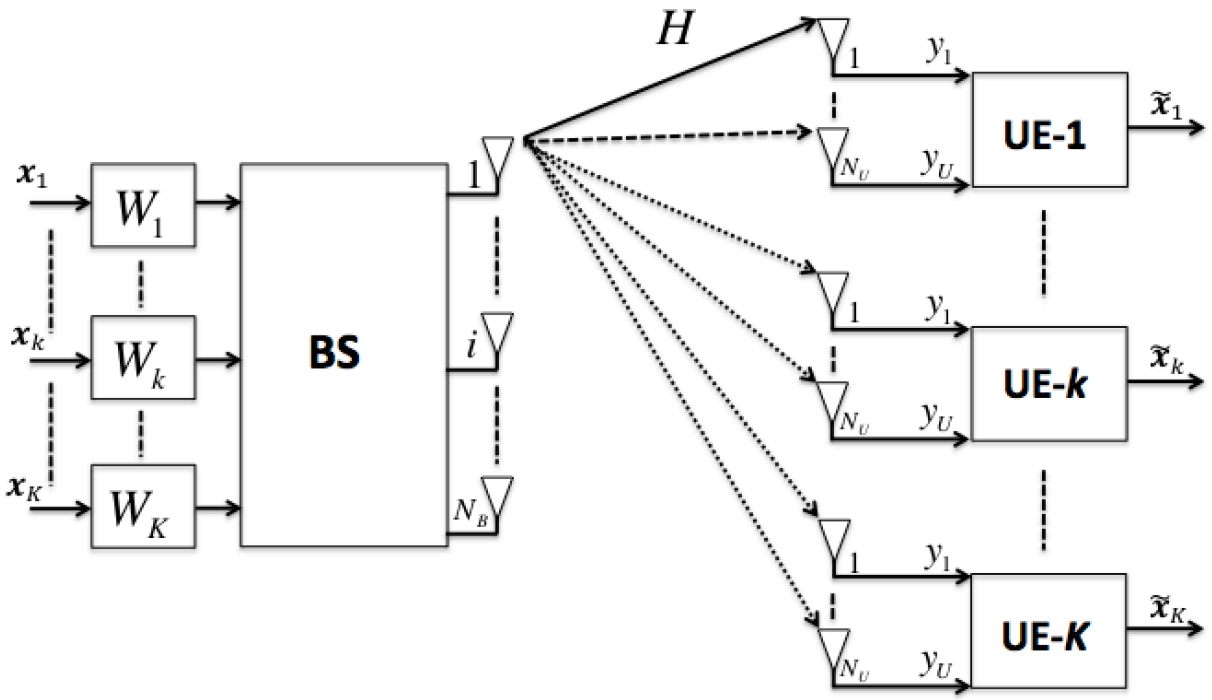

Figure 2: The multi-user multi-input multi-output (MU-MIMO) system model.

The kth UE transmitted and the detected signals are $\boldsymbol{x}_k \in \mathbb{C}^{N_U}$ and $\tilde{\boldsymbol{x}}_k \in \mathbb{C}^{N_U}$ respectively. The channel matrix between the BS and the K users is $\boldsymbol{H} \in \mathbb{C}^{N_R \times N_B}$ which can be expressed as [8]

$$\boldsymbol{H} = [\boldsymbol{H}_1^T \dots \boldsymbol{H}_k^T \dots \boldsymbol{H}_K^T]^T \qquad (5)$$

where the kth element represents the kth UE channel matrix $\boldsymbol{H}_k \in \mathbb{C}^{N_U \times N_B}$. In a flat fading

channel, the received signal $\boldsymbol{y}_k \in \mathbb{C}^{N_U}$ for the kth UE is

$$\boldsymbol{y}_k = \boldsymbol{H}_k \boldsymbol{x}_k + \boldsymbol{H}_k \sum_{j=1, j\neq k}^{K} \boldsymbol{x}_j + \boldsymbol{z}_k \qquad (6)$$

where $\boldsymbol{x}_k \in \mathbb{C}^{N_U}$ is the kth UE transmitted signal, and $\boldsymbol{z}_k \in \mathbb{C}^{N_U}$ is the kth UE AWGN. The term $\boldsymbol{H}_k \sum_{j=1, j\neq k}^{K} \boldsymbol{x}_j$ represents the MUI at the kth UE. To reduce the effect of MUI, channel precoding is employed at the BS. The kth UE precoding matrix can be expressed with $\boldsymbol{W}_k \in \mathbb{C}^{N_B \times N_U}$. From (6), the received signal at the kth UE after channel precoding is [15]

$$\boldsymbol{y}_k = \boldsymbol{H}_k \boldsymbol{W}_k \boldsymbol{x}_k + \boldsymbol{H}_k \sum_{j=1, j\neq k}^{K} \boldsymbol{W}_j \boldsymbol{x}_j + \boldsymbol{z}_k \qquad (7)$$

The goal of precoding is to reduce the effect of the MUI and obtain $\boldsymbol{H}_k \boldsymbol{W}_j = \boldsymbol{0}_{N_U \times N_U}, \forall k \neq j$, where $\boldsymbol{0}_{N_U \times N_U}$ is the zero matrix [17]. From (7), the received signal at the kth UE can be written as

$$\boldsymbol{y}_k = \boldsymbol{H}_k \boldsymbol{W}_k \boldsymbol{x}_k + \boldsymbol{z}_k \qquad (8)$$

After applying channel precoding, the received signal matrix for the K users can be expressed as

$$\begin{bmatrix} \boldsymbol{y}_1 \\ \vdots \\ \boldsymbol{y}_k \\ \vdots \\ \boldsymbol{y}_K \end{bmatrix} = \begin{bmatrix} \boldsymbol{H}_1 \boldsymbol{W}_1 & \cdots & \boldsymbol{0} & \cdots & \boldsymbol{0} \\ \vdots & \ddots & \vdots & \vdots & \vdots \\ \boldsymbol{0} & \cdots & \boldsymbol{H}_k \boldsymbol{W}_k & \cdots & \boldsymbol{0} \\ \vdots & \vdots & \vdots & \ddots & \vdots \\ \boldsymbol{0} & \cdots & \boldsymbol{0} & \cdots & \boldsymbol{H}_K \boldsymbol{W}_K \end{bmatrix} \begin{bmatrix} \boldsymbol{x}_1 \\ \vdots \\ \boldsymbol{x}_k \\ \vdots \\ \boldsymbol{x}_K \end{bmatrix} + \begin{bmatrix} \boldsymbol{z}_1 \\ \vdots \\ \boldsymbol{z}_k \\ \vdots \\ \boldsymbol{z}_K \end{bmatrix} \qquad (9)$$

where the elements of the diagonal matrix represent the product of the UE channel matrix $\boldsymbol{H}_k$ and the UE precoding matrix $\boldsymbol{W}_k$, $k = 1, 2, \ldots, K$. The zeros denote $\boldsymbol{N}_U \times \boldsymbol{N}_U$ zero matrices.

In this report, BD precoding is used to reduce the effect of MUI and decompose the MU-MIMO system into parallel SU-MIMO systems at the BS. Then the detection techniques, which are discussed in the next section, are employed to reduce the inter-antenna interference at each UE [17], [26], [27]. Assume that the number of antennas at the BS is equal to the number of antennas at the K users so that $N_B = N_R = KN_U$. Using singular value decomposition (SVD), the kth UE channel $\boldsymbol{H}_k \in \mathbb{C}^{N_U \times N_B}$ can be represented as [15], [17]

$$\boldsymbol{H}_k = \boldsymbol{U}_k \boldsymbol{\Lambda}_k \boldsymbol{V}_k^H \qquad (10)$$

where the $N_U \times N_U$ matrix $\boldsymbol{U}_k$ and the $N_B \times N_B$ matrix $\boldsymbol{V}_k$ are unitary so that $\boldsymbol{U}_k \boldsymbol{U}_k^H = \boldsymbol{I}_{N_U}$ and $\boldsymbol{V}_k^H \boldsymbol{V}_k = \boldsymbol{I}_{N_B}$. The columns of $\boldsymbol{U}_k$ and $\boldsymbol{V}_k$ are the left singular and right singular vectors of $\boldsymbol{H}_k$, respectively. The columns of $\boldsymbol{U}_k$ are obtained from the eigenvectors of $\boldsymbol{H}_k \boldsymbol{H}_k^H$, while the columns of $\boldsymbol{V}_k$ are obtained from the eigenvectors of $\boldsymbol{H}_k^H \boldsymbol{H}_k$. The $N_{U,k} \times N_B$ matrix $\boldsymbol{\Lambda}_k$ is a diagonal matrix which has non-zero elements only on the diagonal. These elements are the singular values which are the square roots of the eigenvalues of $\boldsymbol{H}_k \boldsymbol{H}_k^H$.

Definition 1: The eigenvalues of an $n \times n$ matrix $\boldsymbol{A}$ are the roots of $det(\boldsymbol{A} - \lambda \boldsymbol{I}_N) = 0$, while the eigenvectors are the non-zero solutions of $(\boldsymbol{A} - \lambda \boldsymbol{I}_N)\vec{\boldsymbol{x}} = 0$. The null space of $\boldsymbol{A}$, which is also called the eigenspace, is the set of solutions of $\boldsymbol{A} - \lambda \boldsymbol{I}_N = 0$.

The $N_B \times N_B$ matrix $\boldsymbol{V}_k$ can be expressed as $\left[\boldsymbol{V}_k^{(1)}\ \boldsymbol{V}_k^{(0)}\right]$, where the matrix $\boldsymbol{V}_k^{(1)} \in \mathbb{C}^{N_B \times (N_B - N_U)}$ consists of the first $(N_B - N_U)$ non-zero singular vectors and $\boldsymbol{V}_k^{(0)} \in \mathbb{C}^{N_B \times N_U}$ is the last N_U zero singular vectors [15]. The non-zero singular vectors and zero singular vectors represent the non-zero solutions and zero solutions of $(\boldsymbol{H}_k - \lambda \boldsymbol{I}_N)\vec{\boldsymbol{x}} = 0$, respectively, as in Definition 1. From (10), the effective channel of the kth UE can be written as

$$\boldsymbol{H}_k = \boldsymbol{U}_k \boldsymbol{\Lambda}_k \boldsymbol{V}_k^H = \boldsymbol{U}_k \boldsymbol{\Lambda}_k \left[\boldsymbol{V}_k^{(1)}\ \boldsymbol{V}_k^{(0)}\right]^H \qquad (11)$$

The $N_B \times N_{U,k}$ matrix $\boldsymbol{V}_k^{(0)}$ forms an orthogonal basis of the null space of $\boldsymbol{H}_k$ [15]. The BD precoding solution is given by

$$\boldsymbol{W}_j = \boldsymbol{V}_k^{(0)}, \forall\, k \neq j \qquad (12)$$

2.2 Signal Detection for Spatial Multiplexing MIMO Systems

In an SM MIMO system, the data stream is divided into multiple streams. These streams are modulated and then transmitted via multiple antennas simultaneously. Although employing SM technology with MIMO systems can increase the system throughput, it also increases the complexity [5]. In this section, four signal detection techniques for SM MIMO systems are discussed. These detection algorithms are zero-forcing (ZF), minimum mean square error (MMSE), ordered successive interference cancellation (OSIC), and maximum likelihood (ML). ZF and MMSE are linear detection techniques. Although, these techniques have low complexity, the performance is worse than with non-linear detection algorithms [3]. OSIC employs either the ZF or MMSE algorithm to detect the received streams one at a time. OSIC detection has better BER performance than ZF or MMSE detection [11]. ML detection provides the best BER performance, but it has the highest computational complexity and so is used as a reference to evaluate the performance of the other techniques. CSI is required at the UE in order to implement these techniques.

2.2.1 Linear Signal Detection Algorithms

Linear detection algorithms apply a weight matrix $\boldsymbol{G}$ to detect the received signal and reduce the inter-antenna interference [5]. Figure 3 shows the linear detection block diagram. The detected signal after applying the weight matrix is

$$\tilde{\boldsymbol{x}} = \boldsymbol{G}\boldsymbol{y} \qquad (13)$$

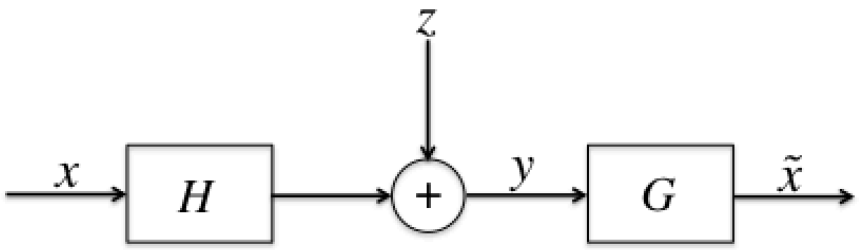

Figure 3: Linear detection block diagram.

In MIMO systems, linear detectors are more practical than nonlinear detectors because of the lower complexity [3]. In general, the computational complexity of a MIMO system increases with the number of antennas. In addition, a large modulation constellation size increases the system complexity. Here, two well known linear detection algorithms, namely zero-forcing (ZF) and minimum mean square error (MMSE), are considered.

2.2.1.1 Zero-Forcing (ZF) Signal Detection

The ZF detector reduces the inter-antenna interference by applying a weight matrix $\boldsymbol{G}_{ZF}$ on the received signal. $\boldsymbol{G}_{ZF}$ is the pseudo inverse of the channel matrix which is given by

$$\boldsymbol{G}_{ZF} = (\boldsymbol{H}^H \boldsymbol{H})^{-1} \boldsymbol{H}^H \qquad (14)$$

and from (2), (13) and (14), the ZF detect or output can be expressed as

$$\tilde{\boldsymbol{x}}_{ZF} = \tilde{\boldsymbol{x}} + (\boldsymbol{H}^H \boldsymbol{H})^{-1} \boldsymbol{H}^H \boldsymbol{z} = \tilde{\boldsymbol{x}} + \tilde{\boldsymbol{z}}_{ZF} \qquad (15)$$

where $\tilde{\boldsymbol{z}}_{ZF} = (\boldsymbol{H}^H \boldsymbol{H})^{-1} \boldsymbol{H}^H \boldsymbol{z}$ is the product of the pseudo inverse of the channel matrix with the AWGN $\boldsymbol{z}$ [3], [17].

2.2.1.2 Minimum Mean Square Error (MMSE) Signal Detection

MMSE is another linear detection technique used to reduce the inter-antenna interference. In contrast to the ZF algorithm, the MMSE algorithm takes the noise term into account and so provides better BER performance. The MMSE detector applies a weight matrix $\boldsymbol{G}_{MMSE}$ to detect the received signal which is given by [3]

$$\boldsymbol{G}_{MMSE} = (\boldsymbol{H}^H\boldsymbol{H} + \sigma_z^2\boldsymbol{I})^{-1}\boldsymbol{H}^H \qquad (16)$$

The MMSE detector requires that the noise variance and channel gain be known at the receiver. From (2), (13) and (16), the MMSE detect or output can be expressed as

$$\tilde{\boldsymbol{x}}_{MMSE} = \tilde{\boldsymbol{x}} + (\boldsymbol{H}^H\boldsymbol{H} + \sigma_z^2\boldsymbol{I})^{-1}\boldsymbol{H}^H\boldsymbol{z} = \tilde{\boldsymbol{x}} + \tilde{\boldsymbol{z}}_{MMSE} \qquad (17)$$

Both the inter-antenna interference and AWGN are considered in the MMSE detector which results in improved performance compared to the ZF detector. Determining $(\boldsymbol{H}^H\boldsymbol{H})^{-1}$ for ZF detection or $(\boldsymbol{H}^H\boldsymbol{H} + \sigma_z^2\boldsymbol{I})^{-1}$ for MMSE detection is the main factor in the computational complexity of these algorithms [25]. The diversity order achieved by these linear detection techniques is $(N_U - N_B + 1)$ [3], [17].

2.2.2 Ordered Successive Interference Cancellation (OSIC) Signal Detection

Successive interference cancellation (SIC) detects the received signal by employing a bank of linear detectors. In this report, SIC employs ZF or MMSE detection. The BER performance of ZF and MMSE signal detection is improved by employing SIC without a significant increase in complexity [17]. SIC detects the parallel received symbols from multiple antennas one at a time. Then it uses the detected symbols for interference cancellation in the next stages. The performance of SIC detection is degraded by error propagation caused by erroneous decisions in previous stages [17].

Ordered successive interference cancellation was proposed to improve SIC detection [11]. OSIC employs ZF or MMSE detection to detect the received symbols at each stage. The received symbols are sorted in descending order based on either the signal-to-noise ratio (SNR) for ZF-OSIC or the signal-to-interference plus noise ratio (SINR) for MMSE-OSIC. The SNR is the ratio of signal power to noise power given by

$$SNR_i = \frac{\mathrm{E}_x \left| \boldsymbol{G}_{i,ZF} \boldsymbol{h}_i \right|^2}{\sigma_z^2 \left\| \boldsymbol{G}_{i,ZF} \right\|^2} \qquad (18)$$

The SINR is the ratio of the signal power to the sum of the power of the other interfering signals (interference power) and noise power given by

$$SINR_i = \frac{\mathrm{E}_x \left| \boldsymbol{G}_{i,MMSE} \boldsymbol{h}_i \right|^2}{\mathrm{E}_x \sum_{j \neq i} \left| \boldsymbol{G}_{i,MMSE} \boldsymbol{h}_j \right|^2 + \sigma_z^2 \left\| \boldsymbol{G}_{i,MMSE} \right\|^2} \qquad (19)$$

where E_x is the energy of the transmitted signal. $\boldsymbol{h}_i$ is the ith column vector of the channel matrix. $\boldsymbol{G}_{i,ZF}$ and $\boldsymbol{G}_{i,MMSE}$ are the ith row of the ZF and MMSE weight matrices, respectively [3], [11],[17]. These vectors are obtained from (14) and (16).

Figure 4 shows the MMSE-OSIC detection procedure for three received symbols. MMSE detection is used at each stage. Assume that the number of antennas at the BS and UE is equal, $N_B = N_U = 3$. There are three received symbols at the UE, where $\boldsymbol{y} = [y_1, y_2, y_3]^T$. Suppose that the received symbols are ordered as y_1, y_2 and y_3 based on the SINR values from (19) so that y_1 has the highest SINR. The MMSE-OSIC detection steps are as follows.

- After ordering the received signal symbols, the first received symbol is detected with the first row vector of the MMSE weight matrix $\boldsymbol{G}_{MMSE}$ in (17). The first detected symbol is given by

$$\tilde{x}_{(1)} = \boldsymbol{G}_{MMSE}(1)\boldsymbol{y} \qquad (20)$$

where $\boldsymbol{G}_{MMSE}(1)$ is the first row of the MMSE weight matrix. Then, the symbol is estimated as the nearest point in the signal constellation. For example, with QPSK modulation, there are four constellation points $-1-j, -1+j, 1-j$, and $1+j$. The function $\mathrm{Q}(\tilde{x}_{(1)})$ estimates the transmitted symbol by determining the nearest constellation point. The first estimated symbol is given by $\hat{x}_{(1)} = \mathrm{Q}(\tilde{x}_{(1)})$.

- In the second stage, the first estimated symbol $\hat{x}_{(1)}$ is used in the interference cancellation which is given by

$$\hat{\boldsymbol{y}}_{(1)} = \boldsymbol{y} - \boldsymbol{h}_{(1)}\hat{x}_{(1)} \qquad (21)$$

where $\hat{\boldsymbol{y}}_{(1)}$ is the received symbols after canceling the first estimated symbol $\hat{x}_{(1)}$. $\boldsymbol{h}_{(1)}$ is the first column of the channel matrix. The OSIC procedure is repeated for the second stage where the second and the third received symbols are ordered based on their SINR values from (19). The second received symbol is detected using MMSE detection as

$$\tilde{x}_{(2)} = \boldsymbol{G}_{MMSE}(2)\hat{\boldsymbol{y}}_{(1)} \qquad (22)$$

where $\boldsymbol{G}_{MMSE}(2)$ is the first row of the MMSE weight matrix which is obtained from (16). Then, the second estimated symbol $\hat{x}_{(2)}$ is determined by $\hat{x}_{(2)} = \mathrm{Q}(\tilde{x}_{(2)})$ as in the previous stage.

- In the last stage, the third received symbol is obtained by canceling the second estimated symbol $\hat{x}_{(2)}$ giving

$$\hat{\boldsymbol{y}}_{(2)} = \hat{\boldsymbol{y}}_{(1)} - \boldsymbol{h}_{(2)}\hat{x}_{(2)} \qquad (23)$$

where $\boldsymbol{h}_{(2)}$ is the second column of the channel matrix. At this stage, there is no need to calculate the SINR. The MMSE is used to detect the third received symbol which is given by

$$\tilde{x}_{(3)} = \boldsymbol{G}_{MMSE}(3)\hat{\boldsymbol{y}}_{(2)} \qquad (24)$$

Then, the third estimated symbol $\hat{x}_{(3)}$ is obtained using the function $\mathrm{Q}(\tilde{x}_{(3)})$ which determines the nearest constellation point.

The performance of the MMSE-OSIC detector is better than that of the MMSE detector when symbols are estimated correctly [3], [11]. The same steps are followed for ZF-OSIC detection but the received symbols are ordered based on their SNR values from (18). Further, ZF detection is used at each stage instead of MMSE detection.

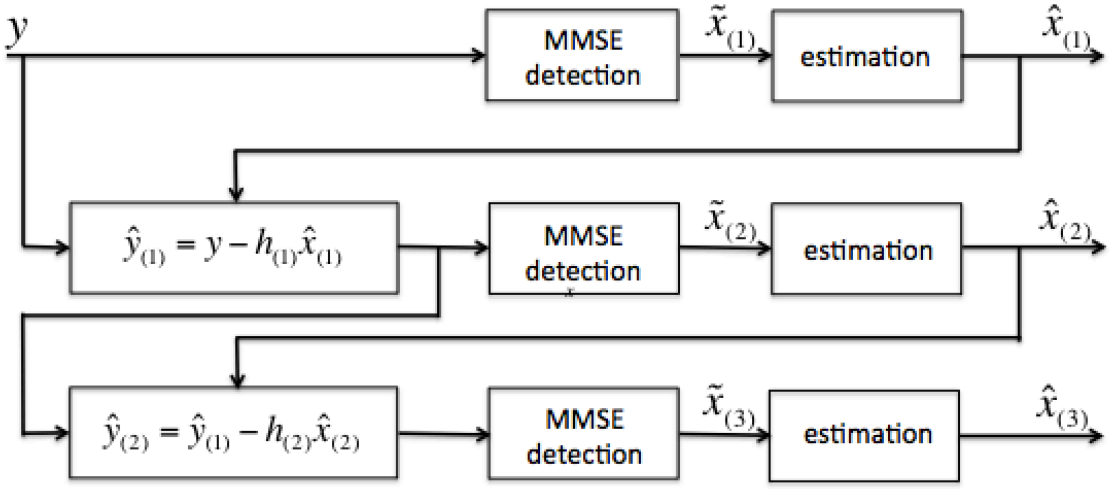

Figure 4: The MMSE-OSIC signal detection block diagram.

The MMSE-OSIC detector provides better performance than the ZF-OSIC detector. The calculation of the SNR or SINR increases the computational complexity of ZF-OSIC and MMSE-OSIC detection compared with ZF and MMSE detection, respectively. The number of SNR or SINR calculations is given by [17]

$$T = \frac{L(L+1)}{2} - 1 \qquad (25)$$

where L is the number of received streams.

2.2.3 Maximum Likelihood (ML) Signal Detection

Maximum likelihood (ML) detection provides the best performance [3], [17]. ML detection estimates the transmitted symbol using an exhaustive search over all possible transmitted symbols, and chooses the one that maximizes the likelihood of the received symbol and has the smallest error probability. The detected signal using the ML detector is given by [3]

$$\tilde{x}_{ML} = arg \max_{x \in M^{N_B}} f(y|x) \qquad (26)$$

where M and N_B are the signal constellation size and number of transmit antennas, respectively. The ML detector calculates the Euclidean distance between the received signal y and all possible transmitted signals x multiplied by the channel matrix $\boldsymbol{H}$, and the detected signal is the one corresponding to the smallest Euclidean distance. The detected signal in (27) can be rewritten as [3]

$$\tilde{x}_{ML} = arg \min_{x \in M^{N_B}} \|y - \boldsymbol{H}x\|^2 \qquad (27)$$

The ML detector employs an exhaustive search over all possible constellation points, which leads to a low error probability but high computational complexity. A large constellation size M and large number of transmit antennas makes ML detection intractable in practical scenarios [3], as the number of Euclidean distance calculations is $|M|^{N_B}$. For example, for a MIMO system with $N_B = 3$ and 16 QAM this number is $16^3 = 4096$. However, ML detection provides optimal performance and achieves a diversity order equal to the number of receive antennas N_U [3], [17]. ML detection is used here as a reference to evaluate the performance of other detection techniques.

2.2.4 Computational Complexity

The detection techniques given previously are now compared in terms of the computational complexity. The computational complexity of ZF, MMSE, and OSIC detection depends on the number of transmit N_B and receive N_U antennas. The complexity of ML detection depends on the modulation constellation size M and the number of antennas at the UE and BS. The computational complexity is measured in terms of the number of floating point operations (FLOPs). A floating-point operation is a mathematical operation that involves floating point numbers. For example, a multiplication followed by an addition requires 2 FLOPs and 8 FLOPs with real values and complex values, respectively [8]. Table 1 gives the number of FLOPs required for the detection algorithms.

Detection Technique	Number of Flops
ZF	$4N_B^3 + 8N_B^2N_U - 2N_U^2$ [18]
MMSE	$4N_B^3 + 8N_B^2N_U$ [25]
ZF-OSIC	$N_B^4 + \left(\frac{5}{2} + \frac{2}{3}N_U\right)N_B^3 + \left(\frac{7}{2} + N_U\right)N_B^2 + \frac{1}{3}N_UN_B$ [20]
MMSE-OSIC	$N_B^4 + \left(\frac{5}{2} + \frac{2}{3}N_U\right)N_B^3 + \left(\frac{7}{2} + N_UN_U^2\right)N_B^2 + \left(\frac{1}{3} + N_U\right)N_UN_B$ [20]
ML	$\lvert M\rvert^{N_B}N_U(N_B + 1)$ [3]

Table 1: Computational complexity for the detection techniques

Figure 5 presents the required number of FLOPs for the detection techniques when the number of antennas at the BS and UE is $N_B = N_U$. This shows that ZF and MMSE detection require the lowest number of FLOPs, while ML detection needs the highest number of FLOPs. The ML detector complexity increases with the constellation size M. This figure also shows that ML detection becomes intractable when 64 QAM is used. Further OSIC detection has lower

complexity than ML detection. For example, the required number of FLOPs for ZF, MMSE, ZF-OSIC and MMSE-OSIC detection when $N_B = N_U = 6$ is 2520, 2592, 3054 and 4566, respectively. For ML detection with $N_B = N_U = 6$ and QPSK, 16 QAM and 64 QAM modulation, the required number of FLOPs is $1720\times10^2, 7046\times10^5$ and 2886×10^9, respectively. The complexity of the ZF-OSIC algorithm depends on the number of SNR calculations, while the MMSE-OSIC algorithm depends on the number of SINR calculations. Thus, the required number of FLOPs for MMSE-OSIC detection is higher than that for ZF-OSIC detection [20].

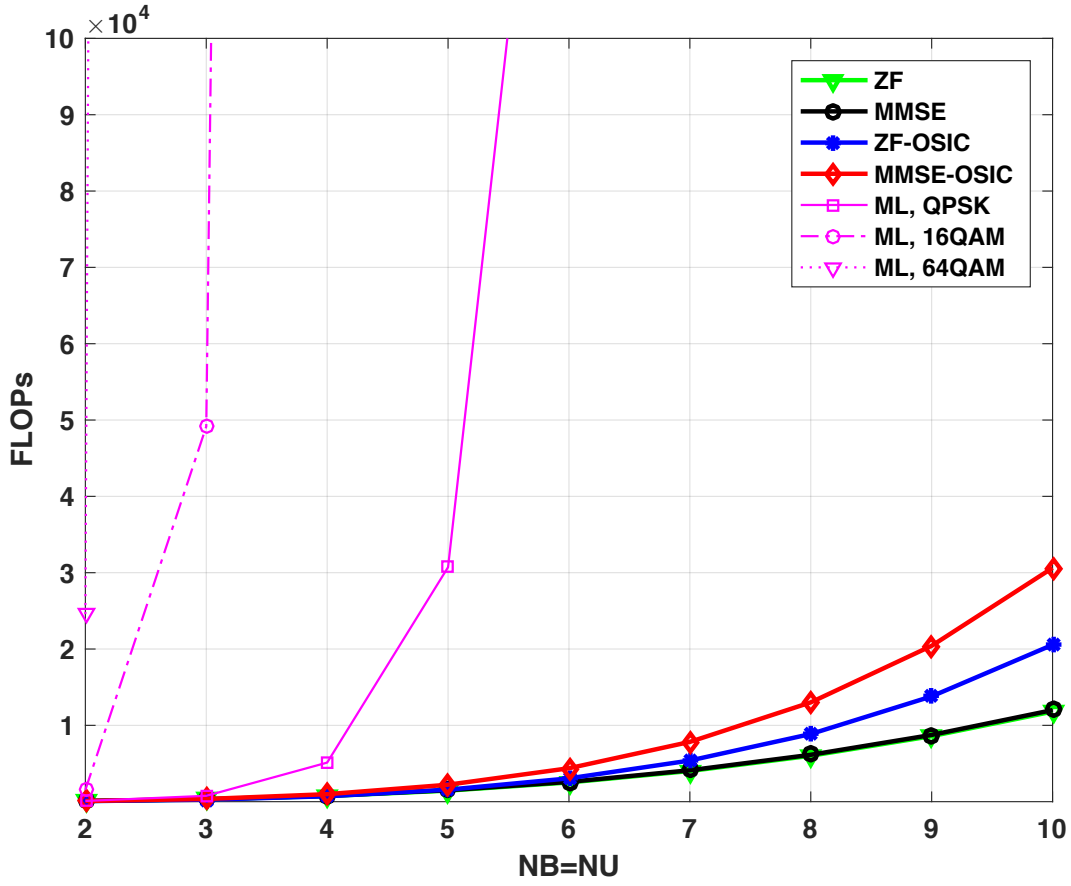

Figure 5: The computational complexity of different detection techniques for MIMO systems with $N_B = N_U$.

2.3 Spatial Correlation

In wireless networks, spatial correlation between antennas occurs due to inadequate antenna spacing and signal scattering [17], which causes a loss in performance. In [6], the Kronecker model was introduced for channel correlation. This model assumes that there is no correlation between the BS and UE due to the distance between them. Thus, there is only correlation between antenna elements at the BS and UE. The Kronecker model for a correlated channel can be expressed as

$$\boldsymbol{H}_{corr} = \boldsymbol{R}_U^{\frac{1}{2}} \boldsymbol{H} \boldsymbol{R}_B^{\frac{1}{2}} \qquad (28)$$

where $\boldsymbol{R}_U$ is the UE correlation matrix, $\boldsymbol{R}_B$ is the BS correlation matrix, and $\boldsymbol{H}$ denotes the channel between the BS and UE. In an urban wireless environment, there can be many obstacles near the UE. Thus, the channels are almost independent when the UE antenna elements are spaced by $\lambda/2$, where λ is the wavelength [17]. Therefore, the spatial correlation is assumed to be zero at the UE, so that $\boldsymbol{R}_U = \boldsymbol{I}_{N_U}$ as in [8], where $\boldsymbol{I}_{N_U}$ is the identity matrix, and from (28)

$$\boldsymbol{H}_{corr} = \boldsymbol{H} \boldsymbol{R}_B^{\frac{1}{2}} \qquad (29)$$

An exponential correlation model was considered in [13] to study the effect of correlation between antenna elements. It was shown that an increase in the exponential correlation coefficient between antenna elements leads to a decrease in system capacity. Thus, increasing the SNR in the case of correlated channels can reduce the loss in system capacity. The correlation matrix elements at the BS is given as [13]

$$\boldsymbol{R}_B(i,j) = \begin{cases} r^{j-i}, & i \leq j \\ r^{i-j}, & i > j \end{cases}, |r| \leq 1 \qquad (30)$$

where r is the correlation between any two neighboring antennas at the BS, $i = 1, 2, \dots, N_B$ and $j = 1, 2, \dots, N_B$. Thus, the correlation is greatest between neighboring antennas. For example, the BS correlation matrix when $N_B = 4$ and $r = 0.7$ from (30) is

$$R_B = \begin{bmatrix} 1 & 0.7 & 0.49 & 0.34 \\ 0.7 & 1 & 0.7 & 0.49 \\ 0.49 & 0.7 & 1 & 0.7 \\ 0.34 & 0.49 & 0.7 & 1 \end{bmatrix}$$

This shows that the correlation between the first and second antennas is greater than the correlation between the first and third antennas. When $r = 0$, the correlation matrix is $\boldsymbol{R}_B = \boldsymbol{I}_{N_B}$ which means there is no correlation between antennas at the BS, so then $\boldsymbol{H}_{corr} = \boldsymbol{H}$. The highest correlation between antennas occurs when $r = 1$. Exponential correlation is used here to study the effect of correlated channels as in [8].

3 Performance Results

3.1 Simulation Models and Parameters

For both SU-MIMO and MU-MIMO systems, the downlink channel model is assumed to be independent and identically distributed (i.i.d.) Rayleigh fading. Perfect channel state information (CSI) is assumed at the BS and UE for MU-MIMO systems, while it is only assumed at the UE for SU-MIMO systems. The BER performance for spatial multiplexing MIMO systems is evaluated. The detection techniques presented in Section 2.2 are employed at the UE. QPSK, 16 QAM, and 64 QAM modulation are employed. Spatial correlation is also considered as discussed in Section 2.3 with different values of r [8], [13]. In this report, the notation $N_B \times N_U$-MIMO is used for SU-MIMO systems, where N_B and N_U are the number of BS and UE antennas, respectively. For MU-MIMO systems, the notation (N_B, K, N_U)-MIMO is used where N_B is the number of BS antennas, K is the number of users, and N_U is the number of UE antennas. The simulation parameters for both SU-MIMO and MU-MIMO systems are listed in Table 2.

The MATLAB simulation steps are summarized below.

1- The transmitted data is generated and then modulated using QPSK, 16 QAM or 64 QAM.
2- The modulated data is divided into multiple data streams based on the MIMO system dimension.
3- The channels are generated based on the number of UE and BS antennas. A Rayleigh fading channel is employed with exponential correlation.
4- BD channel precoding is used on the transmitted streams for MU-MIMO systems.
5- The received signal is the product of the user channel and the transmitted signal. AWGN is added based on the SNR.
6- The UE employs ZF, MMSE, ZF-OSIC, MMSE-OSIC and ML techniques to detect the received signal.
7- The received signal is demodulated and compared to the transmitted data to obtain the BER.

The above steps are repeated for 1000 iterations to obtain the average BER for different SNR values.

SU-MIMO systems $N_B \times N_U$-MIMO	2×2-MIMO, 3×3-MIMO, 4×4-MIMO, 6×6-MIMO
MU-MIMO systems (N_B, K, N_U)-MIMO	$(6, 2, 3)$-MIMO, $(8, 2, 4)$-MIMO, $(12, 2, 6)$-MIMO
Channel model	Rayleigh fading
Data modulation	QPSK, 16 QAM, 64 QAM
Channel information	Ideal (known CSI)
Detection techniques	ZF, MMSE, ML ZF-OSIC, MMSE-OSIC
Spatial correlation	Exponential correlation with $r = 0.5, 0.7$
MU-MIMO channel precoding	BD
Data length per iteration	10000 bits

Table 2: Simulation parameters

3.2 SU-MIMO Performance

The downlink SU-MIMO channel model in Figure 1 is considered where a single BS communicates with a single user. The SU-MIMO channel is assumed to be Rayleigh flat fading. The BS is equipped with $N_B = 2, 3, 4,$ and 6 antennas, and the UE is equipped with the same number of antennas as the BS so that $N_U = N_B$ [3].

The BER performance was evaluated for both uncorrelated and correlated MIMO channels, and QPSK, 16 QAM, and 64 QAM modulation was employed. Figure 6 presents the performance of different detection algorithms for a 2×2-MIMO system. QPSK modulation is used and the channel is uncorrelated. This shows that the ZF detector has the worst performance, while the ML detector has the best. MMSE detection shows an improvement in BER performance compared with ZF detection of approximately 3 dB at a BER of 10^{-3}. Employing ordered successive interference cancellation improves the BER performance of the ZF and MMSE detectors. The ZF-OSIC and MMSE-OSIC detectors have a gain of approximately 3 dB and 2 dB over the ZF and MMSE detectors, respectively, at a BER of 10^{-3}. An SNR of 19 dB is required to achieve a BER of 10^{-3} for the ML detector, while the MMSE-OSIC detector needs an SNR of 26 dB to achieve the same BER.

Figure 7 presents the BER performance of different detection techniques for a 4×4-MIMO system with 16 QAM and an uncorrelated channel. ZF detection still has the worst performance, while ML detection has the best. MMSE detection provides better performance than ZF detection. The required SNR to achieve a BER of 10^{-2} is 28 dB and 30 dB for the MMSE and ZF detectors, respectively. Employing OSIC again provides better performance than the ZF and MMSE techniques with a 2 dB and 2.2 dB gain when the MMSE-OSIC and ZF-OSIC detectors are employed, respectively, at a BER of 10^{-2}. The MMSE-OSIC detector requires an SNR of 26 dB to achieve a BER of 10^{-2}, while the ML algorithm needs an SNR of 19 dB to achieve the same BER. In order to achieve a BER of 10^{-3} instead of 10^{-2}, the ML and MMSE-OSIC detectors require an increase in SNR of 3.2 dB and 9 dB, respectively. Although ML detection provides the best BER performance, it is not practical due to its high computational complexity as mentioned previously.

Figure 8 presents the BER performance of 3×3-MIMO, 4×4-MIMO and 6×6-MIMO systems with QPSK modulation. MMSE, MMSE-OSIC and ML detectors are employed at the UE. This shows that increasing the number of antennas improves the BER performance with ML detection. For example, to achieve a BER of 10^{-3}, there is an approximately 1 dB SNR gain when the number of antennas increases from 3 to 4, and from 4 to 6. The performance remains almost the same as the number of antenna increases with MMSE and MMSE-OSIC detection.

Figures 9 to 11 present the BER performance of a 4×4-MIMO system with ZF, MMSE, and MMSE-OSIC detectors, respectively, with QPSK, 16 QAM, and 64 QAM modulation. Exponential channel correlation is assumed with $r = 0, 0.5$ and 0.7. These results show that the BER performance is better with a modulation scheme that has small constellation size. Figure 11 shows that MMSE-OSIC detection with QPSK has approximately an 8 dB and 15 dB SNR gain compared with 16 QAM and 64 QAM modulation, respectively, at a BER of 10^{-2}. Moreover, there is a noticeable BER performance degradation with exponential channel correlation. The BER performance decreases as r increases. Figure 10 shows that there is approximately a 4 dB of loss with $r = 0.7$ compared with an uncorrelated channel at a BER of 10^{-3} with MMSE detection and QPSK modulation.

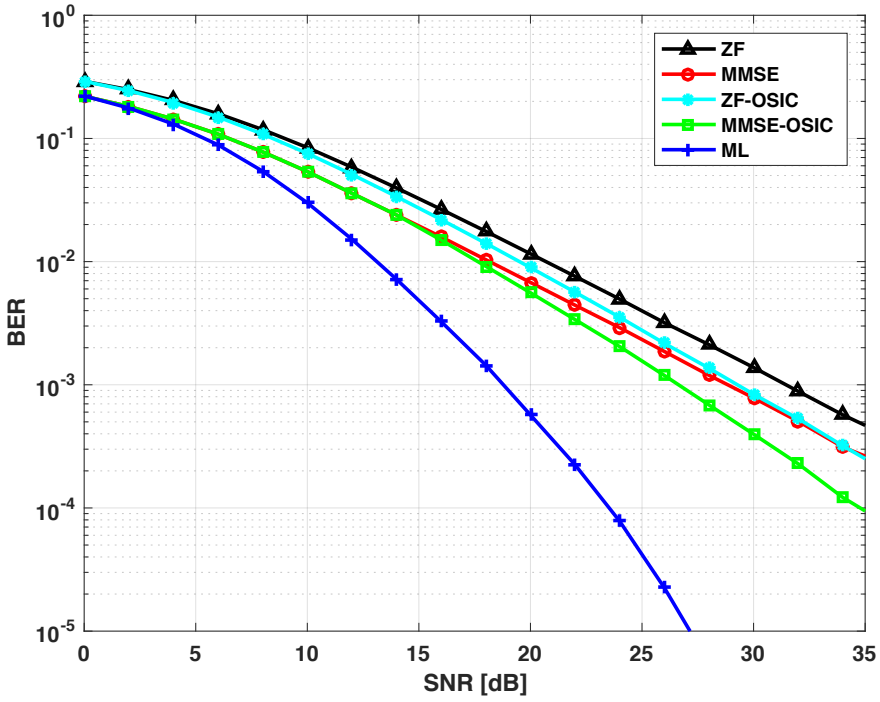

Figure 6: BER performance of a 2×2-MIMO system with QPSK and different detection techniques.

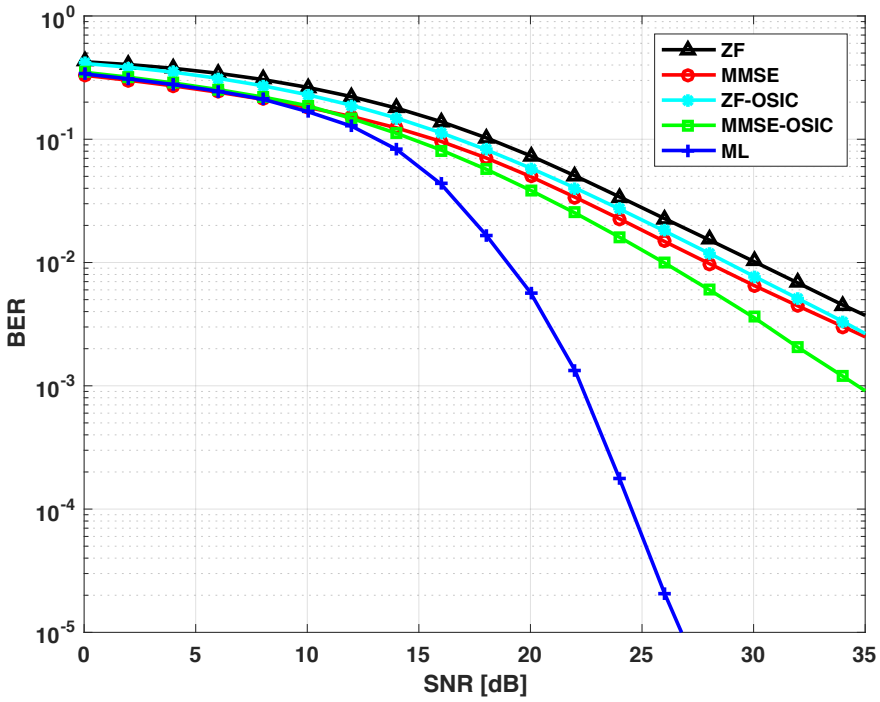

Figure 7: BER performance of a 4×4-MIMO system with 16 QAM and different detection techniques.

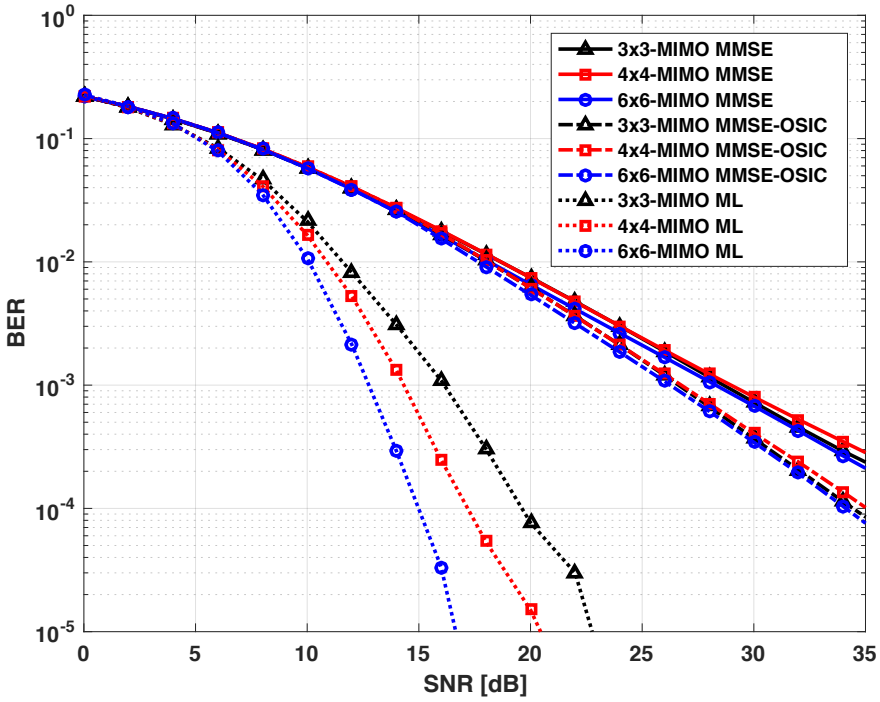

Figure 8: BER performance of SU-MIMO systems with QPSK and different detection techniques.

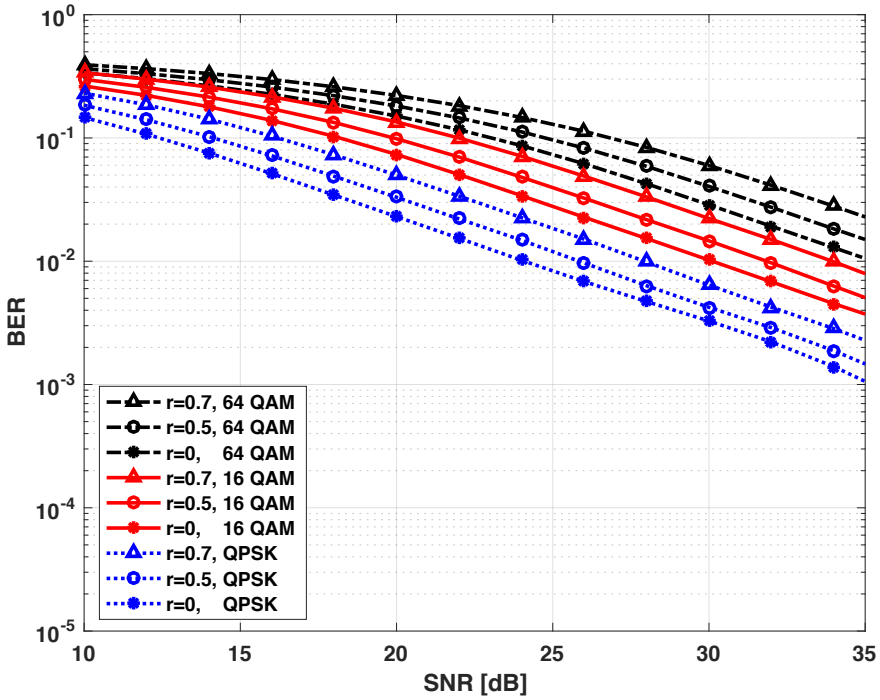

Figure 9: BER performance of a 4×4-MIMO system with a ZF detector and different modulation and correlation coefficients.

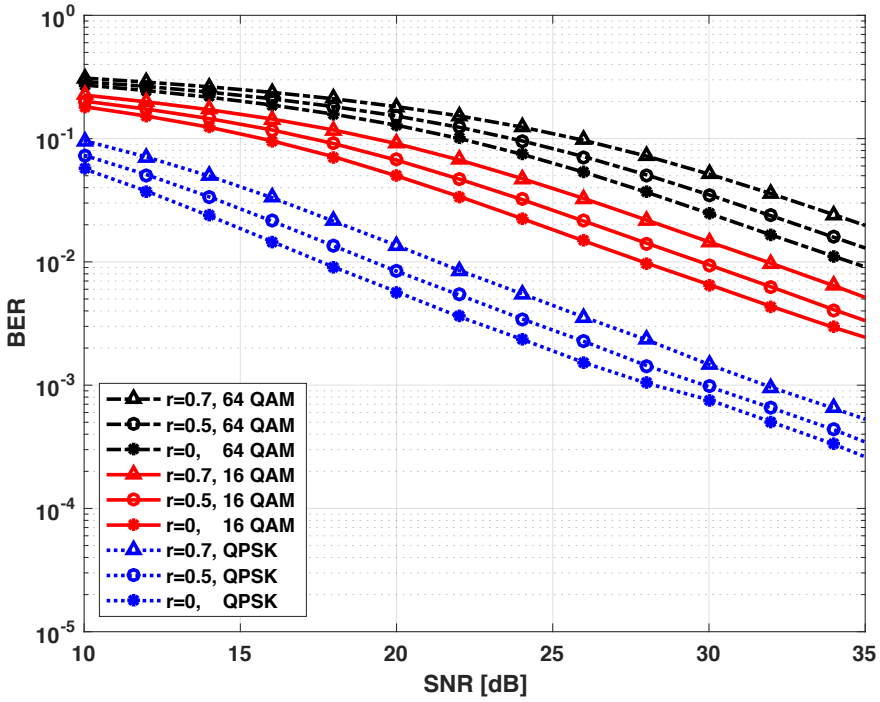

Figure 10: BER performance of a 4×4-MIMO system with an MMSE detector and different modulation and correlation coefficients.

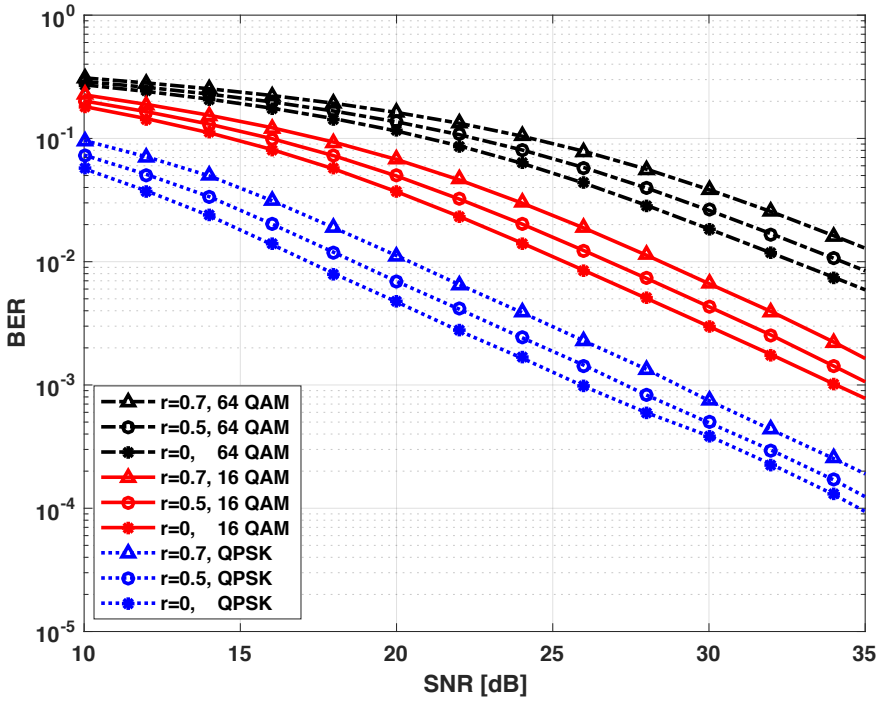

Figure 11: BER performance of a 4×4-MIMO system with an MMSE-OSIC detector and different modulation and correlation coefficients.

3.3 MU-MIMO Performance

The downlink MU-MIMO system in Figure 2 is now considered where a single BS communicates with multiple users over Rayleigh fading channels. The BS is equipped with $N_B = 6, 8,$ and 12 antennas. Two users are assumed and both are equipped with the same number of antennas $N_{U,}$. The number of antennas for both users N_R is assumed to be equal to the number of BS antennas so that $N_R = N_B$. BD precoding is employed at the BS to reduce the MUI and decompose the MU-MIMO system into two parallel SU-MIMO systems.

The BER performance was evaluated for both uncorrelated and correlated channels, and QPSK, 16 QAM, and 64 QAM modulation were employed. Figure 12 presents the performance of different detection techniques for an $(8, 2, 4)$-MIMO system with 16 QAM and uncorrelated channels. This shows that the ZF detector has the worst performance compared to the other detection techniques. MMSE detection provides better performance than ZF detection. The required SNR to achieve a BER of 10^{-2} is 30 dB and 31.8 dB for the MMSE and ZF detectors, respectively. Employing OSIC detection improves the performance of ZF and MMSE detection. Figure 12 shows that the MMSE-OSIC and ZF-OSIC detectors have a gain of approximately 2 dB and 1.5 dB over the MMSE and ZF detectors, respectively, at a BER of 10^{-2}. It also shows that ML detection provides the best performance compared with the other detection techniques. The ML detector requires an SNR of 22 dB to achieve a BER of 10^{-2}, while MMSE-OSIC detection needs an SNR of 28 dB to achieve the same BER. In order to achieve a BER of 10^{-3} instead of 10^{-2}, the ML and MMSE-OSIC detectors require an increase in SNR of 3 dB and 7.5 dB, respectively.

The constellation diagrams in Figures 13 to 17 present the received symbols for an $(8, 2, 4)$-MIMO system with different detection techniques and 16 QAM. These results show that the received symbols are spread around their ideal values due to noise, fading and interference. These symbols are less spread at an SNR of 25 dB compared to 10 dB with ZF and MMSE detection. Figures 13 and 14 show that ZF detection provides worse performance compared with MMSE detection at an SNR of 10 dB with BER of approximately 2.5×10^{-1} and 2.0×10^{-1} respectively. Figures 15 and 16 show that the performance of ZF and MMSE detection improves

at an SNR of 25 dB with BER of approximately 1.9×10^{-2} and 1.5×10^{-2} respectively. Figure 17 shows that ML detection provides the best performance at an SNR of 25 dB where the BER is approximately 3.0×10^{-4}.

Figure 18 presents the BER performance of the MU-MIMO system with $N_B = 6, 8, 12$ antennas and two users, so each user is equipped with $N_U = 3, 4, 6$ antennas. MMSE, MMSE-OSIC and ML detectors are employed at the UE, and QPSK modulation is used. These results show that increasing the number of antennas improves the BER performance with ML detection, while the performance with MMSE and MMSE-OSIC detection remains almost the same.

Figures 19 to 21 present the BER performance of an $(8, 2, 4)$-MIMO system with ZF, MMSE, and MMSE-OSIC detection, respectively, with QPSK, 16 QAM, and 64 QAM modulation. Exponential channel correlation is assumed with $r = 0, 0.5$ and 0.7. These results show that the performance is better when the modulation constellation size is smaller. For example, QPSK provides an approximately 6 dB SNR gain over 16 QAM modulation with a ZF detector for a BER of 10^{-2}. Further, the performance decreases as the exponential correlation increases. Figure 21 shows that there is an approximately 2 dB SNR loss when $r = 0.5$ compared with uncorrelated channels at a BER of 10^{-2} with MMSE-OSIC detection and 16 QAM.

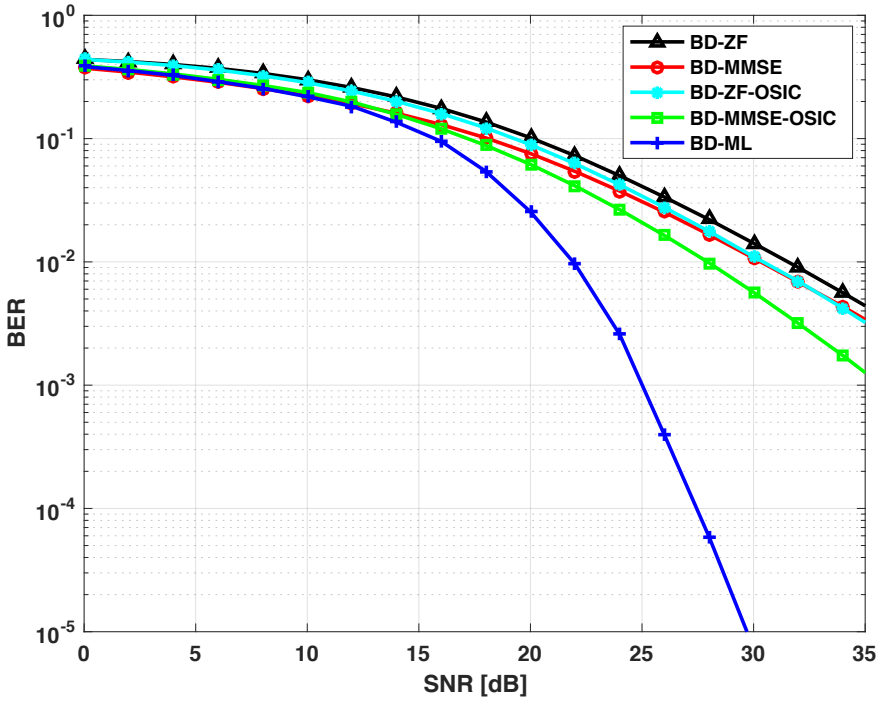

Figure 12: BER performance of an $(8, 2, 4)$-MIMO system with 16 QAM and different detection techniques.

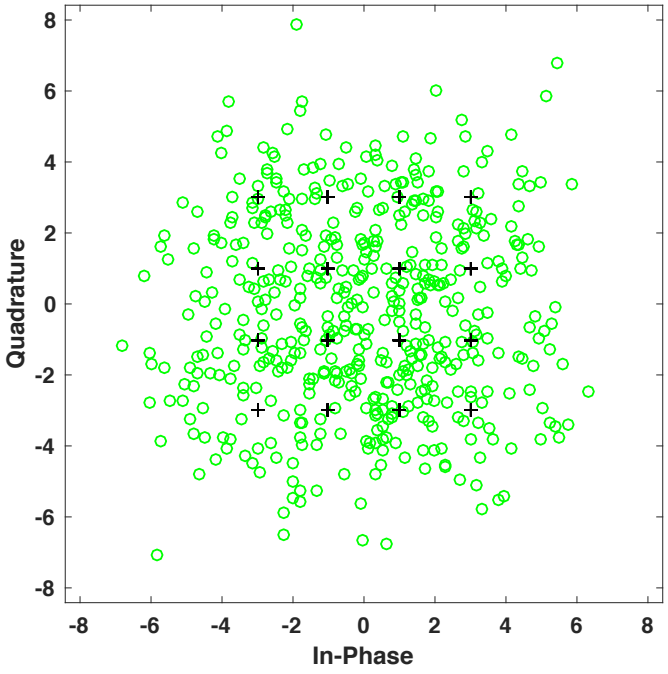

Figure 13: Constellation diagram of the received symbols after ZF detection for 16 QAM and SNR=10 dB.

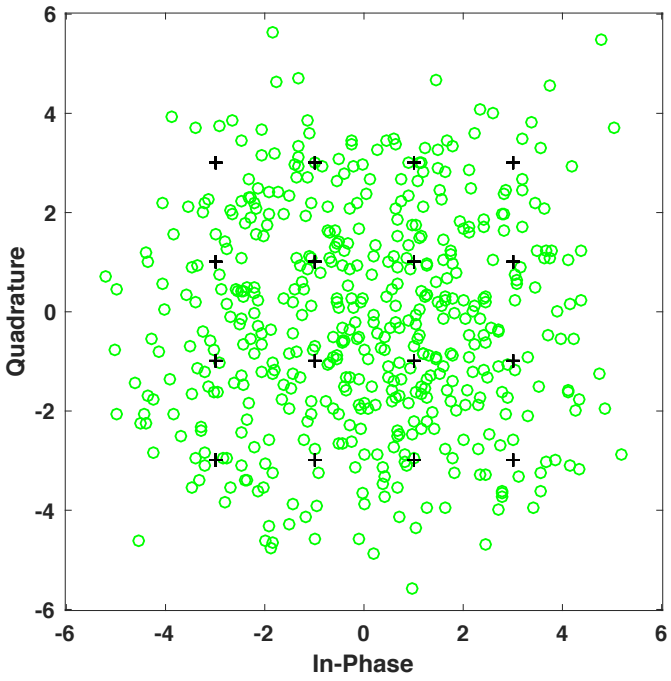

Figure 14: Constellation diagram of the received symbols after MMSE detection for 16 QAM and SNR=10 dB.

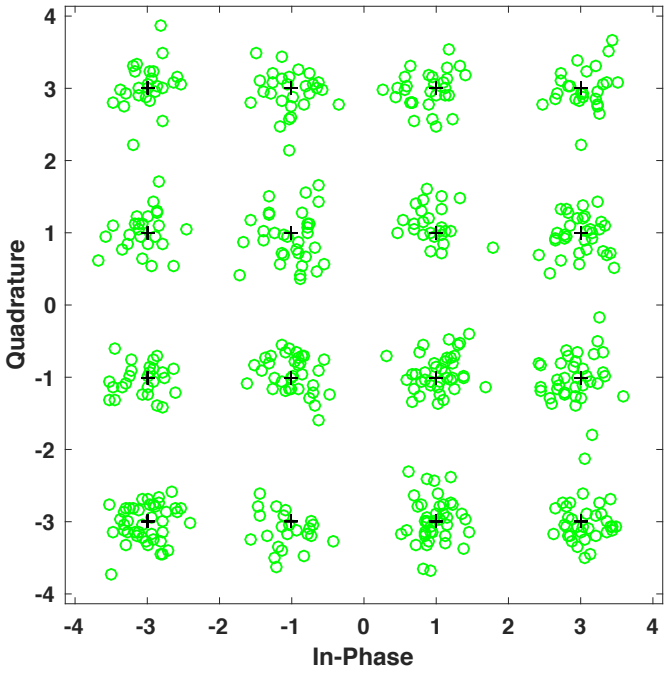

Figure 15: Constellation diagram of the received symbols after ZF detection for 16 QAM and SNR=25 dB.

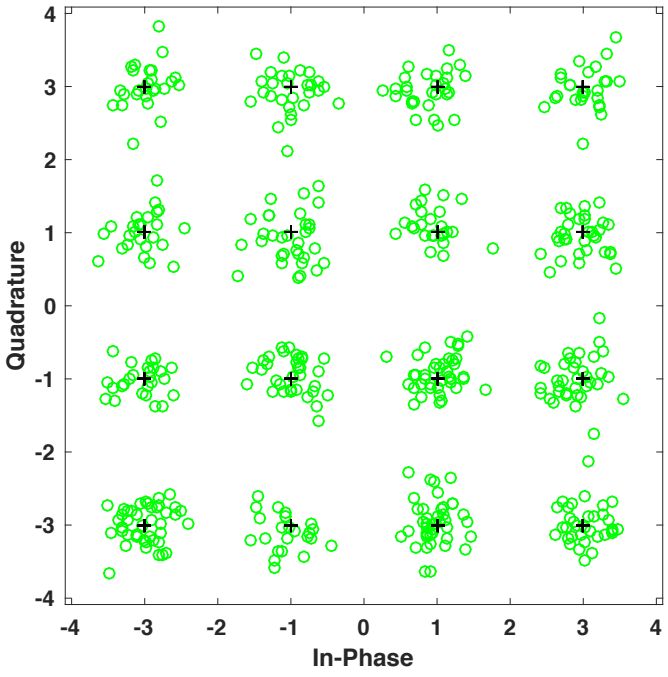

Figure 16: Constellation diagram of the received symbols after MMSE detection for 16 QAM and SNR=25 dB.

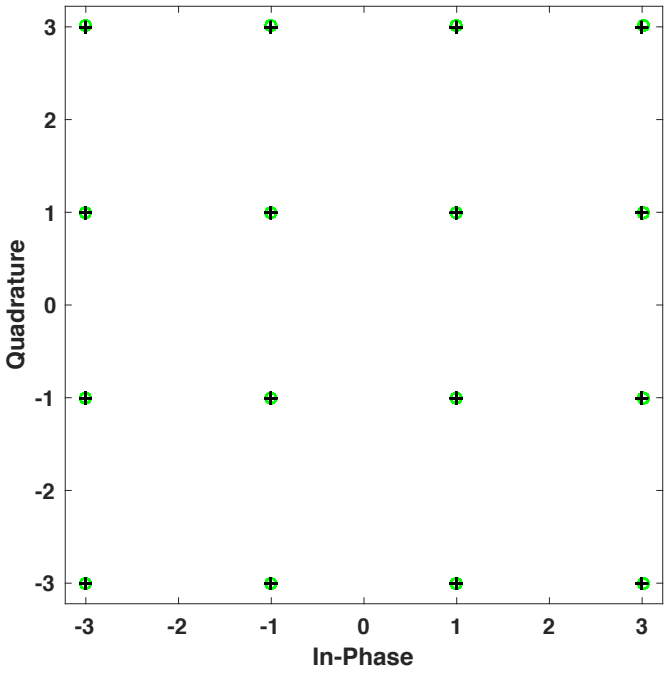

Figure 17: Constellation diagram of the received symbols after ML detection for 16 QAM and SNR=25 dB.

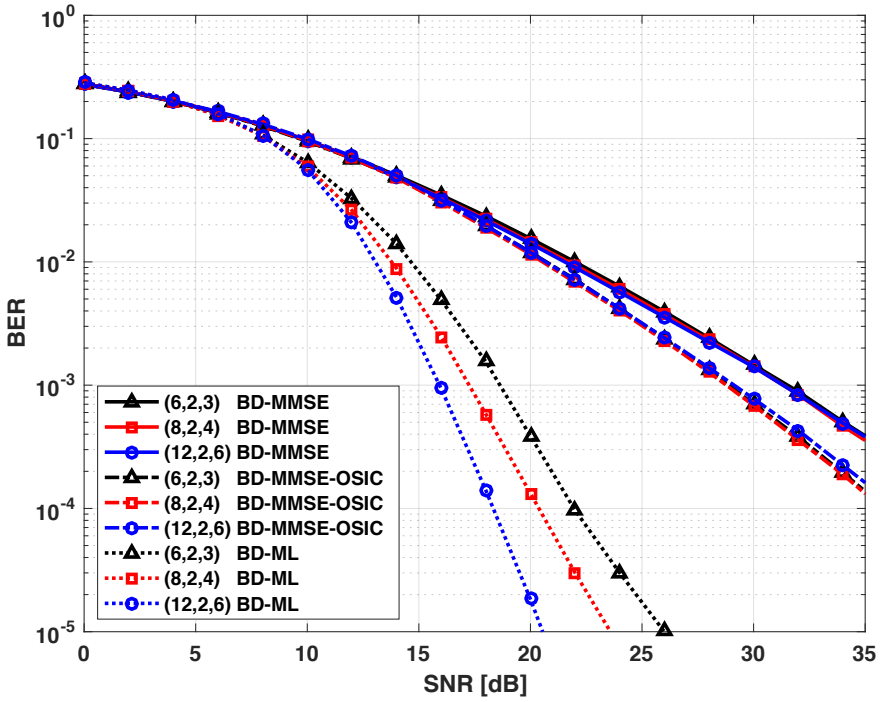

Figure 18: BER performance of MU-MIMO systems with QPSK and different detection techniques.

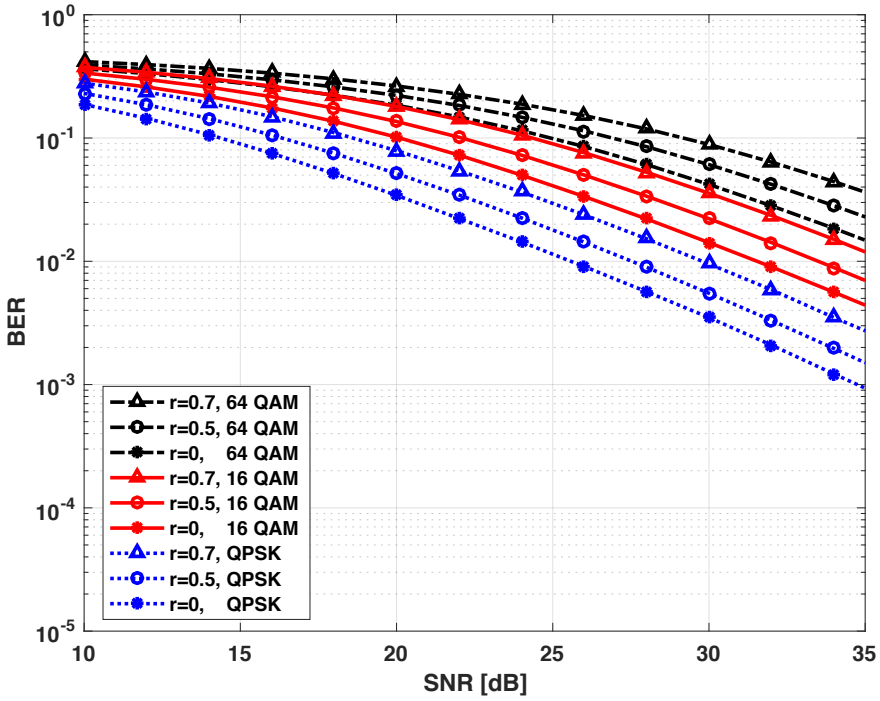

Figure 19: BER performance of an $(8, 2, 4)$-MIMO system with a ZF detector and different modulation and correlation coefficients.

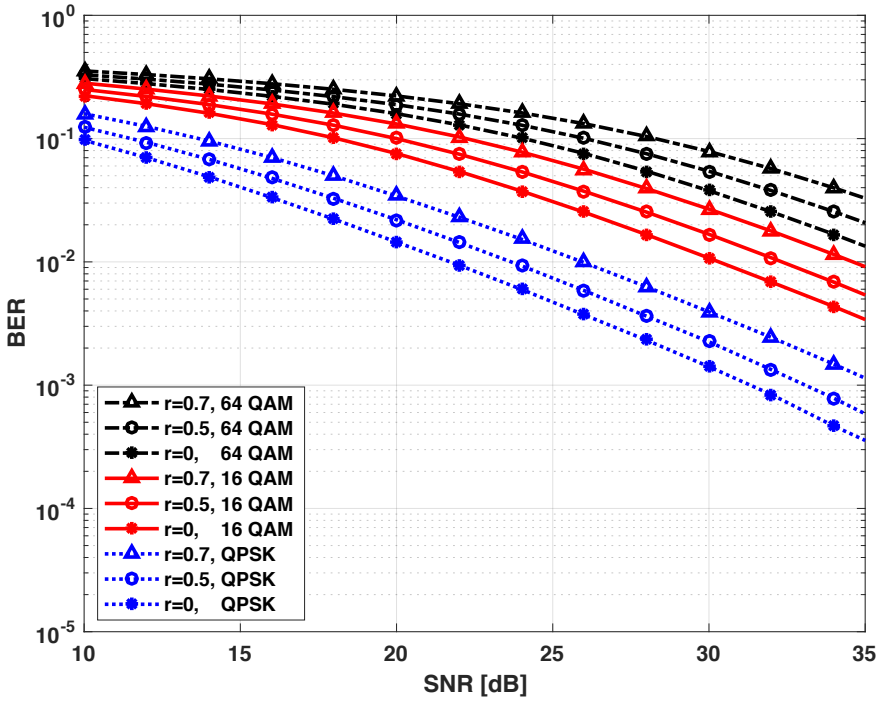

Figure 20: BER performance of an $(8, 2, 4)$-MIMO system with an MMSE detector and different modulation and correlation coefficients.

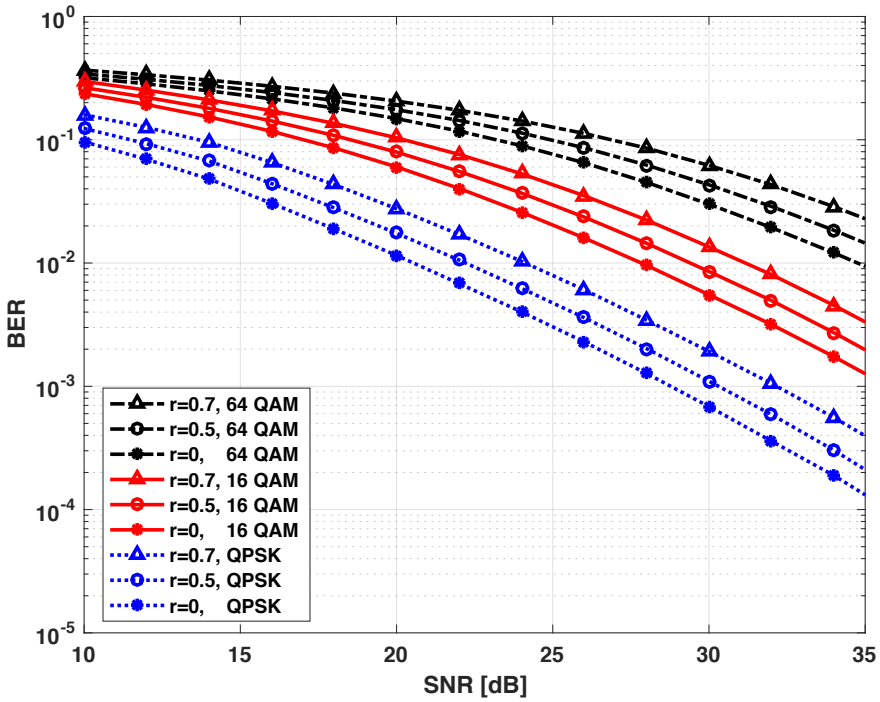

Figure 21: BER performance of an $(8, 2, 4)$-MIMO system with an MMSE-OSIC detector and different modulation and correlation coefficients.

3.4 Discussion

This section discusses the simulation results for SU-MIMO and MU-MIMO systems given in the previous sections.

1- Figures 7 and 12 presented the BER performance of different detection techniques with 4×4-MIMO and $(8,2,4)$-MIMO systems, respectively, and 16 QAM modulation. These show that employing BD precoding successfully decomposed the $(8,2,4)$-MIMO system into two parallel 4×4-MIMO systems. Further, using BD precoding with the $(8,2,4)$-MIMO system reduces the MUI with a small performance degradation compared with the 4×4-MIMO system. This degradation is approximately 1.8, 2.1, 1.6, 2 and 3 dB with the ZF, MMSE, ZF-OSIC, MMSE-OSIC and ML detectors at a BER of 10^{-2}, respectively.

2- OSIC detection provides better BER performance than ZF and MMSE detection.

3- The ML detector provides the best BER performance and outperforms the other detection techniques. However, the complexity of ML detection becomes infeasible from an implementation point of view when the modulation constellation size is large.

4- Figures 8 and 18 showed that increasing the number of antennas with ML detection provides better performance for SU-MIMO and MU-MIMO systems, respectively. In contrast, the performance of the SU-MIMO and MU-MIMO systems with MMSE and MMSE-OSIC detection remains almost the same when the number of antennas increases.

5- A large modulation constellation is affected more by noise, fading and interference as shown in Figures 9 to 11 for a 4×4-MIMO system and Figures 19 to 21 for an $(8,2,4)$-MIMO system. Thus, QPSK provides better BER performance than 16 QAM and 64 QAM.

6- There is a noticeable degradation in BER performance when the channel is spatially correlated. Exponential correlation with different values of r was employed with SU-MIMO and MU-MIMO systems and the results presented in Figures 9 to 11 and Figures 19 to 21, respectively. These show that the BER performance of the detection techniques decreases as the correlation increases.

4 Conclusion and Future Work

Spatial multiplexing MIMO techniques are used to increase the capacity of wireless systems, but they increase the system complexity. This report provided a comparison of the BER performance of zero-forcing (ZF), minimum mean square error (MMSE), ordered successive interference cancellation (OSIC), and maximum likelihood (ML) detection techniques. They were employed at the user equipment (UE) for SU-MIMO and MU-MIMO systems. Block diagonalization (BD) channel precoding was considered at the BS for the downlink MU-MIMO channel. Moreover, spatial correlation and different modulation schemes were considered.

Simulation results were presented which showed that ZF detection has the worst performance while ML detection has the best performance. Employing OSIC provides better BER performance than the ZF and MMSE detection techniques. BD precoding was used to decompose the MU-MIMO system into parallel SU-MIMO systems in order to reduce the multi-user interference (MUI). It was shown that increasing the number of antennas provides diversity gain and improves the performance with ML detection, while the performance with MMSE and OSIC detection techniques remains almost the same as the number of antennas increases. Thus, the system performance can be increased using spatial diversity instead of spatial multiplexing with MIMO systems.

Exponential spatial correlation was also considered for SU-MIMO and MU-MIMO systems. The results obtained show that an increase in the correlation between antennas degrades the BER performance of MIMO systems. Finally, using a small modulation constellation results in better BER performance.

4.1 Future Work

Spatial multiplexing MIMO techniques can be used to increase the channel capacity. In this report, flat fading wireless MIMO channel models were assumed. Thus, spatial multiplexing MIMO system in frequency selective fading could be considered. In addition, the channel state information (CSI) was assumed to be perfectly known which is difficult in practice. Thus, the

BER performance of MU-MIMO systems with BD channel precoding can be studied in the case of imperfect CSI. Currently, massive MIMO where hundreds of antennas are employed is an important research topic. To address the number of antennas, research should be conducted to reduce the complexity of signal detection and channel precoding techniques.

References

[1] A. Goldsmith, Wireless Communications. Cambridge University Press, Cambridge, UK, 2005.

[2] Q. Li, G. Li, W. Lee, M. Lee, D. Mazzarese, B. Clerckx and Z. Li, "MIMO techniques in WiMAX and LTE: A feature overview," IEEE Communications Magazine, vol. 48, no. 5, pp. 86-92, 2010.

[3] L. Bai and J. Choi, Low Complexity MIMO Detection. Boston, MA, USA: Springer, 2012.

[4] E. Telatar, "Capacity of multi-antenna Gaussian channels," European Transactions on Telecommunications, vol. 10, no. 6, pp. 585-595, 1999.

[5] A. Paulraj, R. Nabar and D. Gore, Introduction to Space-time Wireless Communications. Cambridge University Press, Cambridge, UK, 2003.

[6] D. Tse and P. Viswanath, Fundamentals of Wireless Communication. Cambridge University Press, Cambridge, UK, 2005.

[7] C. Peel, B. Hochwald and A. Swindlehurst, "A vector-perturbation technique for near-capacity multiantenna multiuser communication Part I: Channel inversion and regularization," IEEE Transactions on Communications, vol. 53, no. 1, pp. 195-202, 2005.

[8] K. Zu, "Novel efficient precoding techniques for multiuser MIMO systems," Ph.D. thesis, Department of Electronics, University of York, York, UK, 2013.

[9] B. Hassibi and H. Vikalo, "On the sphere-decoding algorithm I. Expected complexity," IEEE Transactions on Signal Processing, vol. 53, no. 8, pp. 2806-2818, 2005.

[10] H. Vikalo and B. Hassibi, "On the sphere-decoding algorithm II. Generalizations, second-order statistics, and applications to communications," IEEE Transactions on Signal Processing, vol. 53, no. 8, pp. 2819-2834, 2005.

[11] T. Im, J. Kim, J. Yi, S. Yun and Y. Cho, "MMSE-OSIC² signal detection for spatially multiplexed MIMO systems," Proc. IEEE Vehicular Technology Conference, pp. 1468-1472, 2008.

[12] M. Khan, K. Cho, M. Lee and J. Chung, "A simple block diagonal precoding for multi-user MIMO broadcast channels," EURASIP Journal on Wireless Communications and Networking, vol. 2014, no. 1, pp. 1-8, 2014.

[13] S. Loyka, "Channel capacity of MIMO architecture using the exponential correlation matrix," IEEE Communications Letters, vol. 5, no. 9, pp. 369–371, 2001.

[14] K. Zu, R. de Lamare and M. Haardt, "Lattice reduction-aided regularized block diagonalization for multiuser MIMO systems," Proc. IEEE Wireless Communications and Networking Conference, pp. 131-135, 2012.

[15] K. Zu, R. de Lamare and M. Haardt, "Generalized design of low-complexity block diagonalization type precoding algorithms for multiuser MIMO systems," IEEE Transactions on Communications, vol. 61, no. 10, pp. 4232-4242, 2013.

[16] L. Boher, R. Legouable and R. Rabineau, "Performance analysis of iterative receiver in 3GPP/LTE DL MIMO OFDMA system," Proc. IEEE International Symposium on Spread Spectrum Techniques and Applications, pp. 103-108, 2008.

[17] Y. Cho, J. Kim, W. Yang and C. Kang, MIMO-OFDM Wireless Communications with MATLAB. Singapore: Wiley, 2010.

[18] Q. Spencer, A. Swindlehurst and M. Haardt, "Zero-forcing methods for downlink spatial multiplexing in multiuser MIMO channels," IEEE Transactions on Signal Processing, vol. 52, no. 2, pp. 461-471, 2004.

[19] J. Kermoal, L. Schumacher, K. Pedersen, P. Mogensen and F. Frederiksen, "A stochastic MIMO radio channel model with experimental validation," IEEE Journal on Selected Areas in Communications, vol. 20, no. 6, pp. 1211-1226, 2002.

[20] M. El-Mashed and S. El-Rabaie, "Signal detection enhancement in LTE-A downlink physical layer using OSIC-based K-best algorithm," Physical Communication, vol. 14, pp. 24-31, 2015.

[21] K. Punia, E. George, K. Babu and G. Reddy, "Signal detection for spatially multiplexed multi input multi output (MIMO) systems," Proc. International Conference on Communications and Signal Processing, pp. 612-616, 2014.

[22] L. Choi and R. Murch, "A transmit preprocessing technique for multiuser MIMO systems using a decomposition approach," IEEE Transactions on Wireless Communications, vol. 3, no. 1, pp. 20-24, 2004.

[23] H. Vikalo, B. Hassibi and T. Kailath, "Iterative decoding for MIMO channels via modified sphere decoding," IEEE Transactions on Wireless Communications, vol. 3, no. 6, pp. 2299-2311, 2004.

[24] S. Sandhu and A. Paulraj, "Space-time block codes: A capacity perspective," IEEE Communications Letters, vol. 4, no. 12, pp. 384-386, 2000.

[25] M. Tuchler, A. Singer and R. Koetter, "Minimum mean squared error equalization using a priori information," IEEE Transactions on Signal Processing, vol. 50, no. 3, pp. 673-683, 2002.

[26] M. Hashem, A. Khan, J. Chung and H. Lee, "Lattice reduction aided with block diagonalization for multiuser MIMO systems," EURASIP Journal on Wireless Communications and Networking, vol. 2015, no. 1, pp. 1-9, 2015.